Comparison of the electronic structure of the Hubbard and $t - J$ models within the cluster perturbation theory

V. I. Kuz'min*
L.V. Kirensky Institute of Physics, SB RAS, 660036 Krasnoyarsk, Russia

S. V. Nikolaev† and S. G. Ovchinnikov‡
Siberian Federal University, 660041 Krasnoyarsk, Russia
and L.V. Kirensky Institute of Physics, SB RAS, 660036 Krasnoyarsk, Russia

(Received 12 May 2014; revised manuscript received 7 November 2014; published 1 December 2014)

Electronic dispersion and density of states (DOS) have been calculated for the Hubbard model and the $t - J$ and $t - J^*$ models with three-site correlated hopping by the cluster perturbation theory. We have found a rather strong quantitative difference both in dispersion and DOS at all doping for the Hubbard and $t - J$ models at the energy scale $\omega \gtrsim t$. The three-site correlated hopping addition results in an almost negligible difference for the Hubbard and $t - J^*$ models. Close to the Fermi energy, at the scale $\omega \lesssim J$, the electronic structure of all three models is similar. We have found the line of zeros of the Green function for the $t - J$ model that has been previously obtained for the Hubbard model by cellular dynamical mean-field theory calculations.

DOI: 10.1103/PhysRevB.90.245104 PACS number(s): 71.10.Hf, 71.30.+h, 74.72.−h

I. INTRODUCTION

The discovery of high-T_c cuprates has resulted in intensive studies of the electronic structure of doped Mott insulators. Experimental data have revealed the emergence of non-Fermi liquids under a radical evolution of electronic structure upon doping. The most unusual state found in a wide doping range between a weakly doped insulator and overdoped Fermi liquid is the pseudogap state. The origin of the pseudogap state is still an unresolved problem. The two-dimensional (2D) Hubbard model is a relevant low-energy model for cuprates. For this model, the pseudogap was reproduced in various theories [1,2]. The arclike angle-resolved photoemission spectra (ARPES) were reproduced by the cluster perturbation theory (CPT) [3], dynamical cluster approximation (DCA) [4], and the cellular dynamical mean-field theory (CDMFT) [5–7]. Two Lifshitz transitions with changes of the Fermi-surface topology have been found using CPT calculations [8]. Since short-range correlations form a very important ingredient of physics in doped 2D Mott insulators, cluster extensions of single-site approaches such as dynamical mean-field theory (DMFT) [9] are important.

A widely spread simplification of the Hubbard model is the $t - J$ model obtained by eliminating the excitations over the Mott-Hubbard gap U in the limit $U \gg t$, where t is the nearest-neighbor hopping parameter [10–12]. Decreasing the number of local single-electron states in the $t - J$ model remarkably reduces the computational efforts in the CPT for the $t - J$ model. It should be noted that the unitary transformation of the Hubbard model Hamiltonian results in the so-called $t - J^*$ model. The $t - J^*$ Hamiltonian has an additional three-site correlated hopping H_3 above the $t - J$ Hamiltonian. On the mean-field level, the H_3 term results in a renormalization of hopping $\propto t^2/U$. That is why quite often it is neglected and one obtains the $t - J$ model. For example, different forms of the $t - J$ model are analyzed in Ref. [13]. Nevertheless, there are some indications that the H_3 term may be important in the formation of the superconducting state with d-wave symmetry [14,15].

We would like to clarify the relevance of the models discussed here to cuprates. The Hubbard model has three energy scales: the high energy of the Coulomb parameter U, the intermediate energy of the interatomic hopping t ($t \ll U$), and the low-energy scale of the exchange interaction $J \sim t^2/U$. The energy U determines the Mott-Hubbard gap between the upper Hubbard band (UHB) and the lower Hubbard band (LHB) and is irrelevant for cuprates due to the charge-transfer origin of the insulator gap [16]. Thus, eliminating the UHB in the $t - J$ model leaves two scales, t and J, in which both are low energy vs U. The lowest scale J determines the carrier dispersion close to the Fermi level and the Fermi-surface topology. The bandwidth scale t is relevant to the high-energy ARPES observations such as high-energy kinks and waterfalls [17–19]. That is why the electronic structure of the $t - J$ and Hubbard models is of interest both at the J and t scales.

In this paper, we compare the band dispersion and DOS in the normal phase of the Hubbard model and the $t - J$ model within the CPT approach and find that the differences for these two models become negligibly small when taking into account the H_3 term. It means that the Hubbard model and the $t - J^*$ model provide indeed similar electronic structure, while the electronic structure of the $t - J$ model at the high-energy scale $\omega \gtrsim t$ differs remarkably from the one obtained within the Hubbard model. As concerns the low-energy scale $\omega \lesssim J$, all three models give similar results. Our other finding is zeros of the Green function for the $t - J$ and $t - J^*$ models that were obtained earlier for the Hubbard model [6,7].

*valippkuz@gmail.com
†25sergeyn@mail.ru
‡sgo@iph.krasn.ru

II. MODEL AND METHOD

The Hubbard model [20] in the nearest-neighbor hopping approximation is given by the Hamiltonian

$$H = \sum_{i,\sigma}\left\{(\varepsilon-\mu)n_{i,\sigma} + \frac{U}{2}n_{i,\sigma}n_{i,\bar{\sigma}}\right\} - t\sum_{\langle i,j\rangle,\sigma} a^{\dagger}_{i,\sigma}a_{j,\sigma}, \quad (1)$$

where $a^{\dagger}_{i\sigma}$ and $a_{i\sigma}$ are the creation and annihilation operators of the electron with spin σ on the site i, $\bar{\sigma} = -\sigma$, $n_{i\sigma} = a^{\dagger}_{i\sigma}a_{i\sigma}$ is the particle-number operator, μ is the chemical potential, U is the Coulomb repulsion parameter, t is the hopping amplitude, and ε is the one-particle energy.

A canonical transformation in the limit $U \gg t$ leads to the following Hamiltonian [12]:

$$H_{t-J^*} = H_{t-J} + H_3, \quad (2)$$

$$H_{t-J} = -t\sum_{\langle i,j\rangle,\sigma}(c^{\dagger}_{i,\sigma}c_{j,\sigma} + \text{H.c.}) + J\sum_{\langle i,j\rangle}\left(\mathbf{S}_i\mathbf{S}_j - \frac{n_i n_j}{4}\right), \quad (3)$$

$$H_3 = -\frac{t^2}{U}\sum_{i,\sigma}\sum_{\delta\neq\delta'}(c^{\dagger}_{i+\delta,\sigma}n_{i,\bar{\sigma}}c_{i+\delta',\sigma} - c^{\dagger}_{i+\delta,\sigma}c^{\dagger}_{i,\bar{\sigma}}c_{i,\sigma}c_{i+\delta',\bar{\sigma}}), \quad (4)$$

where $J = 4t^2/U$, $\mathbf{S}_i$ is the spin operator, and the creation $c^{\dagger}_{i,\sigma}$ and annihilation $c_{i,\sigma}$ operators obey the anticommutation relations [21,22]

$$\{c_{i,\sigma}, c^{\dagger}_{j,\sigma'}\} = \delta_{ij}\left[\delta_{\sigma\sigma'}(1-n_{i,\bar{\sigma}}) + (1-\delta_{\sigma\sigma'})S^{-\sigma}_i\right], \quad (5)$$

$$\{c^{\dagger}_{i,\sigma}, c^{\dagger}_{j,\sigma'}\} = \{c_{i,\sigma}, c_{j,\sigma'}\} = 0, \quad (6)$$

where $S^{\sigma}_i = a^{\dagger}_{i\sigma}a_{i\bar{\sigma}}$ is a spin-flip operator.

We cover a 2D square lattice by translations of 2×2 cluster using the method similar to Ref. [23] and study a paramagnetic solution. There are three different types of three-site correlated hopping: between sites of a single cell, two cells, or three different cells. Taking this into account, one can regroup the terms in Eq. (2) in order to divide the intracluster interactions from the intercluster. After applying an exact diagonalization to the Hamiltonian of an isolated cluster, one can define X operators, $X^{\alpha} \equiv X^{p,q} = |p\rangle\langle q|$ [24]. Here, $|p\rangle$ and $\langle q|$ are local eigenstates. In terms of X operators, Eq. (2) takes the form

$$H = \sum_{f,p}E_p X^{p,p}_f + \sum_{f,\Delta i,\alpha,\beta}[t_{\alpha,\beta}(f,f+\Delta i) + t^*_{\alpha,\beta}(f,f+\Delta i)]X^{\alpha}_f X^{\beta}_{f+\Delta i} + \sum_{f,\Delta i,\lambda,\lambda'}w_{\lambda,\lambda'}(f,f+\Delta i)X^{\lambda}_f X^{\lambda'}_{f+\Delta i} + \sum_{f,\Delta i,\Delta j,\alpha,\lambda,\beta}t^*_{\alpha,\beta,\lambda}(f,f+\Delta i,f+\Delta j) \times X^{\alpha}_f X^{\lambda}_{f+\Delta i}X^{\beta}_{f+\Delta j}. \quad (7)$$

Here, E_p is an energy of cluster state $|p\rangle$, $t_{\alpha,\beta}(f,f+\Delta i)$, $t^*_{\alpha,\beta}(f,f+\Delta i)$, and $w_{\lambda,\lambda'}(f,f+\Delta i)$ are matrix elements in X representation of the terms in Eq. (2), which are responsible for hopping, three-site interactions, and exchange, respectively, matrix elements $t^*_{\alpha,\beta,\lambda}(f,f+\Delta i,f+\Delta j)$ correspond to correlated three-site hopping between three different clusters, α and β are Fermi type, and λ and λ' means the Bose-type root vectors [25].

Considering intercluster interactions as a perturbation within Hubbard-I approximation, one has a typical CPT equation [26] for the Green function $D_{\alpha,\beta}(\tilde{\mathbf{k}},\omega) = \langle\langle X^{\alpha}_{\tilde{\mathbf{k}}}|X^{-\beta}_{\tilde{\mathbf{k}}}\rangle\rangle_{\omega}$ in the momentum representation:

$$\widehat{D}^{-1}(\tilde{\mathbf{k}},\omega) = [\widehat{D}^0(\omega)]^{-1} - \widehat{V}(\tilde{\mathbf{k}}), \quad (8)$$

where

$$\widehat{V}(\tilde{\mathbf{k}}) = \widehat{T}(\tilde{\mathbf{k}}) + \widehat{T}^*(\tilde{\mathbf{k}}) + \widehat{J}, \quad (9)$$

$$D^0_{\alpha,\beta}(\omega) = \frac{F(\alpha)}{\omega-\Omega(\alpha)}\delta_{\alpha,\beta}, \quad (10)$$

$$\Omega(\alpha) = E_q(N+1) - E_p(N) - \mu, \quad (11)$$

$$F(\alpha) \equiv F(p,q) = \langle X^{p,p}\rangle + \langle X^{q,q}\rangle. \quad (12)$$

In Eq. (9), $\widehat{T}(\tilde{\mathbf{k}})$, $\widehat{T}^*(\tilde{\mathbf{k}})$, and $\widehat{J}$ are the matrices of hopping, three-site interactions, and exchange, respectively. In Eqs. (10)–(12), $\widehat{D}^0(\tilde{\mathbf{k}},\omega)$ is the exact local Green function and $F(\alpha)$ is the occupation factor. Wave vector $\tilde{\mathbf{k}}$ belongs to the reduced Brillouin zone.

The relation between the Green function in X representation and the Green function $D_{\alpha\beta}(\tilde{\mathbf{k}},\omega)$ that is defined on the original lattice reads [27,28]

$$G_{\sigma}(\mathbf{k},\omega) = \frac{1}{N_c}\sum_{\alpha,\beta}\sum_{i,j=1}^{N_c}\gamma_{i,\sigma}(\alpha)\gamma_{j,\sigma}(\beta)\,e^{-i\mathbf{k}(\mathbf{r_i}-\mathbf{r_j})} \times D_{\alpha,\beta}(\tilde{\mathbf{k}},\omega), \quad (13)$$

where $\mathbf{k}$ belongs to the original Brillouin zone and equation $D_{\alpha,\beta}(\tilde{\mathbf{k}},\omega) = D_{\alpha,\beta}(\mathbf{k},\omega)$ is taken into account [27]. N_c is the number of sites within a cluster and it is equal to four in our case; $\gamma_{i,\sigma}(\alpha)$ are the matrix elements of $c_{i,\sigma}$ in X representation.

The X-operator representation allows one to construct the norm-conserving version of CPT, i.e., the NC-CPT introduced in Ref. [28] and applied to the Hubbard model. According to the mentioned paper, we define the f factor in order to keep control over the total quasiparticle spectral weight:

$$f \equiv \frac{\sum_{\alpha}|\gamma_{i,\sigma}(\alpha)|^2 F(\alpha)}{(1+p)/2}, \quad (14)$$

where the hole-doping rate p defines an electron concentration $\langle n_{i\sigma}\rangle = \frac{1-p}{2}$.

The spectral function satisfies the equation

$$\int d\omega A_{\sigma}(\mathbf{k},\omega) = \langle\{c_{\mathbf{k},\sigma}, c^{\dagger}_{\mathbf{k},\sigma}\}\rangle = f(1+p)/2. \quad (15)$$

When accounting for all possible Hubbard quasiparticles, $f = 1$. It is possible to reduce the Hilbert-space dimension by neglecting some high-energy cluster states that reduce the f factor. The following results are obtained with $f \geqslant 0.995$, thus we can significantly reduce the computational time without

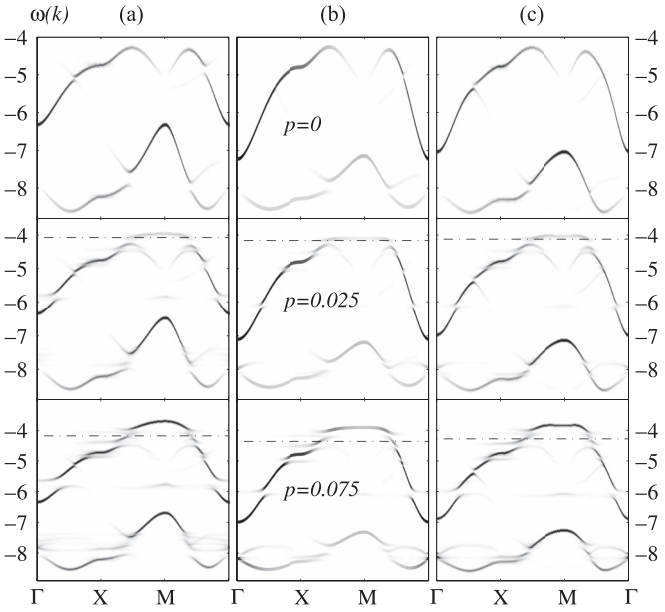

FIG. 1. Doping-dependent evolution of dispersion $\omega(\mathbf{k})$ (in t units) of the LHB in (a) the $t-J$ model, (b) the Hubbard model, and (c) the $t-J^*$ model at $U=12$. Here and below, the dash-dotted line denotes the chemical potential, $\Gamma=(0,0)$, $X=(\pi,0)$, $M=(\pi,\pi)$, energy is measured in units of next-neighbor hopping, and p is the doping concentration.

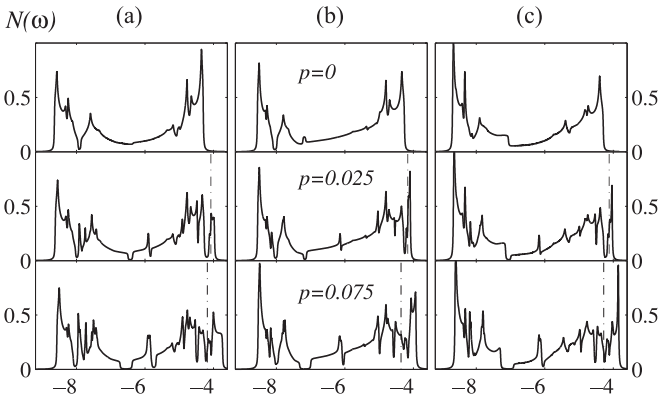

FIG. 2. Doping dependence of DOS $N(\omega)$ of the LHB in (a) the $t-J$ model, (b) the Hubbard model, and (c) the $t-J^*$ model at $U=12$.

any notable influence on the output. We dope holes in the way similar to Ref. [23]. The Hilbert space of a 2×2 cluster is divided into the subspaces with different numbers of electrons N within a cluster. Next, the occupancy of the ground states in the subspaces with $N=4$ and $N=3$ is defined as $1-x$ and x, respectively. In our case, $x=4p$ and maximum doping is 0.25.

III. RESULTS

Our results for the spectral function distribution at $U=12$ are shown in Fig. 1. Figure 1(b) shows typical features of the lower Hubbard band (LHB): minor spectral weight around (π,π), the appearance of in-gap states with doping, the saddle point at $(\pi,0)$, and the presence of a high-energy subband, which have been observed previously within different cluster theories [29,30]. Note that the upper Hubbard band (UHB, not present here) and LHB resulting from splitting of the single-electron band due to strong correlation in the simplest Hubbard-I-like approximation are split further due to high-order corrections, as was shown by several methods [31–33].

Comparing Fig. 1(a) with Fig. 1(b), one can notice rather strong quantitative differences in the dispersion of the Hubbard and $t-J$ models. The LHB consists of several subbands with different momentum-dependent spectral weight, as has been shown earlier by the quantum Monte Carlo [31] and variational CPT (V-CPT) [32] calculations. In the $t-J$ model, these subbands have approximately the same width, and in the Hubbard model, the upper subband is wider than the lower subband. As a consequence, one can observe an appearance of the gap close to $\omega=-7t$ in the Hubbard model [Fig. 2(b)] and nearby $\omega=-6.5t$ in the $t-J$ model [Fig. 2(a)]. In the upper part of Fig. 1, it is clear that the $t-J$ model at the point (π,π) (M point) results in a state much higher in energy [Fig. 1(a)] (more than t) than the one in the Hubbard model [Fig. 1(b)]. The in-gap states band curve near the M point is quite flat in the Hubbard model, as distinct from the curve with a clearly defined maximum in the $t-J$ model. Furthermore, there is a specific intensive band curve segment about the M point in the $t-J$ model [Fig. 1(a)], in contrast to the noticeably less intensive analogous segment in the Hubbard model [Fig. 1(b)]. Note that the decrease of the intensity of the spectral weight near the M point in the Hubbard model is due to the presence of UHB and the corresponding weight transfer between bands [23]. But in the $t-J$ model, the spectral weight does not flow from LHB and the intensity of the part of the dispersion near the M point will always be higher than the one in the Hubbard model.

Taking the H_3 term into account leads to the almost identical dispersion both in the Hubbard model and the $t-J^*$ model, as can be seen by comparing Fig. 1(b) with Fig. 1(c). One can also notice the quantitative agreement in the gap location in DOS in the Hubbard [Fig. 2(b)] and the $t-J^*$ [Fig. 2(c)] models. Unlike the $t-J$ model in the M point, the $t-J^*$ model gives the energy [Fig. 1(c)] the same as the Hubbard model [Fig. 1(b)]. Analogous to the comparison of the results of the Hubbard and $t-J$ models (see above), there is a difference in the magnitude of the quasiparticle spectral weight near the M point in the Hubbard and $t-J^*$ models.

Note that despite the differences in the high-energy region of the electronic spectrum for $U=12$, the dispersion near the Fermi level is similar for all models. Moreover, we presented results for the broadening parameter $\delta=0.01t$, which allowed one to see the fine structure of the electronic spectrum [23], but which is significantly smaller than the experimental energy resolution in ARPES. The result of this comparison is not trivial and suggests that the use of these models is justified to describe the low-energy spectral properties of the hole-doped cuprates. But this is not true for the high-energy region of the electronic spectrum, where the $t-J$ model should not be used, as follows from our results.

The differences in the electronic structure at $U=6$ are similar to those described above. It can be seen in Figs. 3(a) and 4(a) that there is a large number of breaks in dispersion in the $t-J$ model, which are absent in the Hubbard model. As one can see in Figs. 3(c) and 4(c), such breaks are eliminated

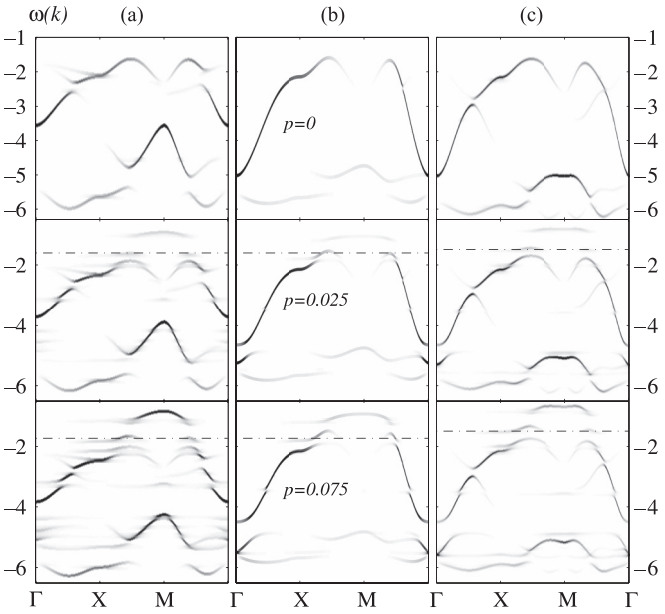

FIG. 3. The same as in Fig. 1 at $U = 6$.

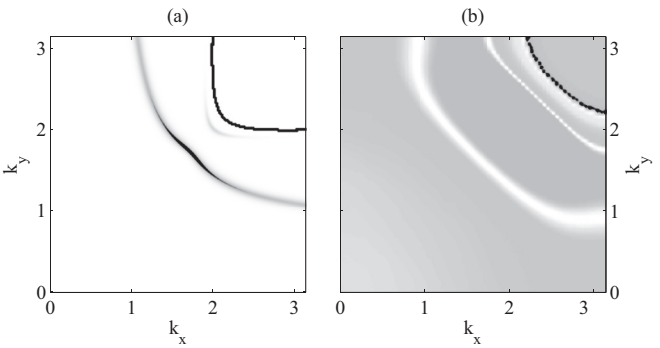

FIG. 5. The spectral weight distribution in the first quadrant of the Brillouin zone at Fermi energy and line of zeros (black solid curve) in the $t - J$ model at $t' = -0.12t, t'' = 0.15t, J = 0.295t$, where t' and t'' are the hopping integrals, respectively, between sites of second and third coordinate spheres. The doping $p = 0.14$ and the broadening $\delta = 0.01t$. (a) The real part of the Green function $\mathrm{Re}[G_\sigma(\mathbf{k},\omega)^{-1}]$ in the Hubbard model at $U = 8t$, $p = 0.11$ taken from Ref. [7]. (b) The white regions correspond to poles of the Green function and the black curve corresponds to zeros.

by taking the H_3 term into account. Also, the distribution of the spectral weight between the subbands is reproduced in the $t - J^*$ model similar to the Hubbard model, in contrast to the $t - J$ model (see Fig. 3). At the given value of the Coulomb repulsion, the renormalization of hopping leads to the existence of the local minimum with major spectral weight at point (π,π) [see Fig. 3(c)]. However, there is a maximum at this point in the Hubbard model. Thus, it shows that the $t - J^*$ model has minor differences from the Hubbard model for small U. On the other hand, the dispersion within the $t - J$ model has significant differences, indicating that it is not fully suitable for the description of the electronic structure at the corresponding U.

CDMFT calculations [6,7] have revealed the lines of zeros of the Green function at Fermi energy or the so-called Luttinger surface [34] in the Hubbard model. The nonuniform spectral weight distribution on the Fermi surface is a consequence of the location of the lines of zeros close to the lines of poles of the Green function. The coexistence of poles and zeros and their reconstruction with doping seems to play an important role in the physics of doped Mott insulators. Figure 5(a) shows our results for the $t - J$ model, which are in qualitative agreement with the data obtained in Ref. [7] [see Fig. 5(b)]. Note that at the Fermi level, the $t - J$ and $t - J^*$ models for the set of parameters in Fig. 5 give similar results for the band structure. So the distribution of zeros of the Green function in the $t - J^*$ model is the same as in the $t - J$ model. Therefore, we represent the results for the $t - J$ model only. The spectral weight distribution along the arc has a maximum in a nodal direction. The proximity of zeros to poles leads to the minor spectral weight of the segment of the Fermi surface closer to (π,π). This circumstance explains the absence of this segment in ARPES experiments.

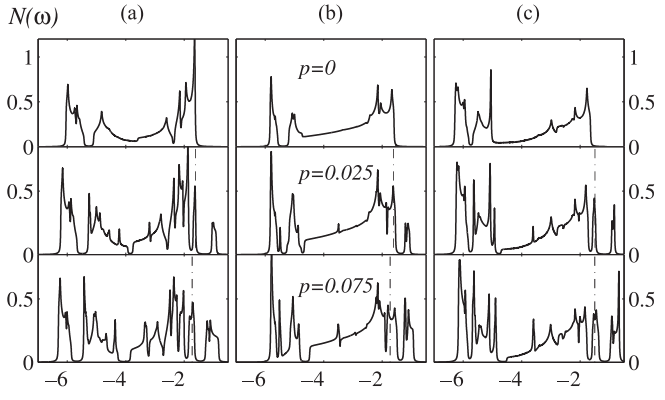

FIG. 4. The same as in Fig. 2 at $U = 6$.

IV. CONCLUSIONS

In conclusion, we have shown that taking three-site correlated hopping into account in the $t - J$ model leads to an almost negligible difference in the electronic structure of the $t - J^*$ model and the Hubbard model, contrary to the standard $t - J$ model. The exact determination of the wave function of two electrons on the 2D square lattice [35] shows that there are no bound states in the Hubbard model. However, a bound state does exist at any finite U in the whole Brillouin zone in the $t - J$ model. In the $t - J^*$ model, there is no bound state around point (π,π) for any finite U and there is no bound state in the whole Brillouin zone at $U > 8t$. Thus, one has to consider three-site interactions in the effective Hamiltonian to reproduce the physics of the Hubbard model. Our approximate consideration of the many-electron problem agrees with the given conclusion. In addition, our approach allowed us to reveal the lines of zeros of the Green function in the $t - J$ model and show their influence on the spectral weight distribution along the Fermi surface. In particular, we found a segment of the Fermi surface with minor spectral weight around point (π,π) at doping concentration $p = 0.14$ and showed that the decreasing of spectral weight depends

straightforwardly on the proximity of lines of zeros to lines of poles. It should be noticed that we observe such behavior in the $t - J$ and $t - J^*$ models, while the analogous result has been found for the Hubbard model in the framework of CDMFT [6,7] and NC-CPT [23].

The study of the high-energy electronic structure is very important for the explanation of the high-energy anomalous properties in cuprates. It is known that the ARPES has revealed the high-energy kink (HEK) in the dispersion. Furthermore, the HEK is observed in a broad range of doping in cuprates [17–19]. The theoretical study of this question has been made in many works, both within the Hubbard model [36] and the $t - J$ model [37]. However, there is disagreement between the results of these models. The HEK in a broad range of doping is well observed within the Hubbard model. But the $t - J$ model results in the HEK for a hole-doped system only. Our results show that this disagreement is possibly due to neglecting the three-site correlated hopping in the $t - J$ model.

ACKNOWLEDGMENTS

This work is supported by RFBR (Grants No. 13-02-01395-a, No. 14-02-31677-mol-a, and No. 14-02-00186-a), the Ministry of Education and Science of Russia (Government Contract No. 3085, SibFU 2014 GF-2), and a grant of the Russian President (Grant No. NSh-2886.2014.2).

[1] R. Preuss, W. Hanke, and W. von der Linden, Phys. Rev. Lett. **75**, 1344 (1995).
[2] Y. Yanase *et al.*, Phys. Rep. **387**, 1 (2003).
[3] D. Senechal and A.-M. S. Tremblay, Phys. Rev. Lett. **92**, 126401 (2004).
[4] A. Macridin, M. Jarrell, T. Maier, P. R. C. Kent, and E. D'Azevedo, Phys. Rev. Lett. **97**, 036401 (2006).
[5] M. Civelli, M. Capone, S. S. Kancharla, O. Parcollet, and G. Kotliar, Phys. Rev. Lett. **95**, 106402 (2005).
[6] T. D. Stanescu and G. Kotliar, Phys. Rev. B **74**, 125110 (2006).
[7] S. Sakai, Y. Motome, and M. Imada, Phys. Rev. Lett. **102**, 056404 (2009).
[8] S. Ovchinnikov, M. Korshunov, S. Nikolaev, E. Shneyder, and A. Krinitsyn, J. Supercond. Nov. Magn. **26**, 2831 (2013).
[9] A. Georges, G. Kotliar, W. Krauth, and M. J. Rozenberg, Rev. Mod. Phys. **68**, 13 (1996).
[10] L. N. Bulaevskii, E. L. Nagaev, and D. I. Khomskii, JETP **27**, 836 (1968).
[11] J. E. Hirsch, Phys. Rev. Lett. **54**, 1317 (1985).
[12] K. A. Chao, J. Spalek, and A. M. Oles, J. Phys. C: Condens. Matter **10**, 271 (1977).
[13] J. Jedrak and J. Spalek, Phys. Rev. B **83**, 104512 (2011).
[14] J. E. Hirsch, Phys. Lett. A **136**, 163 (1989).
[15] V. V. Valkov, T. A. Val'kova, D. M. Dzebisashvili, and S. G. Ovchinnikov, JETP Lett. **75**, 378 (2002).
[16] J. Zaanen, G. A. Sawatzky, and J. W. Allen, Phys. Rev. Lett. **55**, 418 (1985).
[17] T. Valla, T. E. Kidd, W.-G. Yin, G. D. Gu, P. D. Johnson, Z.-H. Pan, and A. V. Fedorov, Phys. Rev. Lett. **98**, 167003 (2007).
[18] F. Schmitt, B. Moritz, S. Johnston, S.-K. Mo, M. Hashimoto, R. G. Moore, D.-H. Lu, E. Motoyama, M. Greven, T. P. Devereaux, and Z.-X. Shen, Phys. Rev. B **83**, 195123 (2011).
[19] I. M. Vishik, N. Barisic, M. K. Chan, Y. Li, D. D. Xia, G. Yu, X. Zhao, W. S. Lee, W. Meevasana, T. P. Devereaux, M. Greven, and Z.-X. Shen, Phys. Rev. B **89**, 195141 (2014).
[20] J. Hubbard, J. Proc. Roy. Soc. A **276**, 238 (1963).
[21] J. Spalek, Acta Phys. Pol. A **111**, 409 (2007).
[22] S. G. Ovchinnikov and V. V. Val'kov, *Hubbard Operators in the Theory of Strongly Correlated Electrons* (Imperial College Press, London-Singapore, 2004).
[23] S. V. Nikolaev and S. G. Ovchinnikov, JETP **114**, 118 (2012).
[24] J. Hubbard, J. Proc. Roy. Soc. A **285**, 542 (1965).
[25] R. O. Zaitzev, JETP **43**, 574 (1976).
[26] D. Senechal, D. Perez, and D. Plouffe, Phys. Rev. B **66**, 075129 (2002).
[27] T. Maier, M. Jarell, T. Pruschke, and M. H. Hettler, Rev. Mod. Phys. **77**, 1027 (2005).
[28] S. V. Nikolaev and S. G. Ovchinnikov, JETP **111**, 635 (2010).
[29] D. Senechal, D. Perez, and M. Pioro-Ladriere, Phys. Rev. Lett. **84**, 522 (2000).
[30] M. Civelli, Phys. Rev. B **79**, 195113 (2009).
[31] C. Grober, R. Eder, and W. Hanke, Phys. Rev. B **62**, 4336 (2000).
[32] C. Dahnken, M. Aichhorn, W. Hanke, E. Arrigoni, and M. Potthoff, Phys. Rev. B **70**, 245110 (2004).
[33] A. S. Krinitsyn, S. V. Nikolaev, and S. G. Ovchinnikov, J. Supercond. Nov. Magn. **27**, 955 (2014).
[34] I. Dzyaloshinskii, Phys. Rev. B **68**, 085113 (2003).
[35] V. V. Val'kov and V. A. Mitskan, Phys. Met. Metallogr. **100**, 10 (2005).
[36] B. Moritz, F. Schmitt, W. Meevasana, S. Johnston, E. M. Motoyama, M. Greven, D. H. Lu, C. Kim, R. T. Scalettar, Z.-X. Shen, and T. P. Devereaux, New J. Phys. **11**, 093020 (2009).
[37] M. M. Zemljic, P. Prelovsek, and T. Tohyama, Phys. Rev. Lett. **100**, 036402 (2008).